ISSN(Online): 2319-8753
ISSN (Print): 2347-6710

International Journal of Innovative Research in Science, Engineering and Technology

(An ISO 3297: 2007 Certified Organization)

Vol. 4, Issue 12, December 2015

Multifunctional Materials of Polyurethane/Buckypaper for Structural Vibration Damping and Strain Sensing

Weiwei Lin[1], Yonatan Rotenberg[3], Hadi Fekrmandi[4], Kevin P. Ward[3], Cesar Levy [2]

Graduate Student, Department of Mechanical and Materials Engineering, Florida International University, Miami, FL, USA[1]

Professor, Department of Mechanical and Materials Engineering, Florida International University, Miami, FL, USA[2]

Undergraduate Student, Department of Mechanical and Materials Engineering, Florida International University, Miami, FL, USA[3]

Graduate Student, Applied Research Center, Florida International University, Miami, FL, USA[4]

ABSTRACT: A Polyurethane/Buckypaper sensor was prepared by curing polyurethane upon Buckypaper. Cantilever beam free vibration test method was adopted to investigate the damping properties of such composites. It was found that the damping ratio of the Polyurethane/Buckypaper composites is higher than each of their individual components. Also, the location of the sample vis-à-vis the location of the cantilever beam's fixed support played a very important part in the damping ratio. Tests results showed that when the sensor is placed at the clamped end for both single side attached and double sided attachment, the damping ratios are 1.6-2.1 times higher than their counterpart values for beams clamped at the free, uncovered end. Also, the double sided attachment model has higher damping ratio compared with single sided attachment model. Furthermore, the static tensile strain sensing and the dynamic strain sensing tests results showed that the PU/Buckypaper sensor has linear strain sensing capabilities and has the ability to dynamically sense input signals well, and therefore, has the potential to serve as a generalized lightweight sensor.

KEYWORDS: Polyurethane, Buckypaper, Damping properties, Strain sensing properties.

I. INTRODUCTION

Multifunctional materials promise more weight-efficient, volume-efficient performance flexibility and potentially less maintenance than traditional multicomponent brass-board systems, which attracted many researchers' interests these years. For example, it is beneficial and crucial to enable critical infrastructures, including aircraft, ships, highways, bridges, buildings, and pipelines, both with damping and strain sensing properties. For this reason, these infrastructures are sometimes subjected to severe loading conditions due to hurricanes, earthquakes and other natural disasters during their lifetime. Multifunctional materials having damping properties can prevent or at least minimize catastrophic failures and subsequent loss of life, while strain sensing property materials provide further inspection and evaluation of the problems caused through these disasters[1]].

In recent times, the damping properties of multiwall carbon nanotubes (MWCNT) films have attracted much attention. Research has demonstrated that a thin layer of MWCNT deposited by chemical vapor deposition method (CVD) and sandwiched between two silicon substrates can dramatically increase the damping ratio and stiffness of the sandwich structure simultaneously [2]. Theoretical analysis also showed that the addition of CNTs into a polymer matrix can improve the damping ratio and stiffness of the matrix [3], while experiments of different MWCNT composite films verified the theoretical prediction [4]. Furthermore, MWCNT films have been demonstrated to show the capability of being strain sensors [5].

ISSN(Online): 2319-8753
ISSN (Print): 2347-6710

International Journal of Innovative Research in Science, Engineering and Technology

(An ISO 3297: 2007 Certified Organization)

Vol. 4, Issue 12, December 2015

Polyurethane (PU) has unique dynamic properties in combination with its high load-bearing capacity, properties which were broadly studied for vibration control applications. Studies have been completed testing the damping properties of MWCNT in PU matrix, for example, [6]. However, due to the large aspect ratio of the CNTs, the dispersion and directional alignment of the MWCNTs in the polymer matrix is still a great challenge.

Herein, a layer by layer attachment method was employed to make PU/Buckypaper composites. A free vibration test method was adopted to study their damping properties. Static and dynamic strain sensing properties were also investigated. One of the advantages of such a composite sensor is its light weight compared to a passively constrained layer damper.

II. EXPERIMENTAL SECTIONS

A. Preparation of Pu/Buckypaper

Buckypaper was bought from Nano-lab (Newton, MA, www.nano-lab.com). The procedures to make Buckypaper is briefly summarized in the succeeding paragraphs.

MWCNTs was purified by placing into the mixed acids (hydrochloric acid (HCl) and the nitric acid (H_2SO_4)) to remove the catalyst iron particles. The MWCNTs were then washed with deionized water until they were neutralized. Then, the material was filtered, dried and reground into powder. Nanosperse AQ, which is a surfactant was added into MWCNTs in order to form a stable suspension. Finally, the suspension was pressed through a filter, resulting in the MWCNTs as residual film on the filter surface. The Buckypaper was obtained when peeled from the filter surface.

The Buckypaper was made of hollow-structured MWCNTs with 15±5 nm outer diameter, about 5-20 microns in length and purity higher than 95%. The thickness of the MWCNT film was around 100 micron and the relative density was about 50%. The Buckypaper was cut into 3.5 cm ×0.9 cm×100 μm sections and placed into 6 cm ×1.3 cm×0.3 cm glass mold very closely.

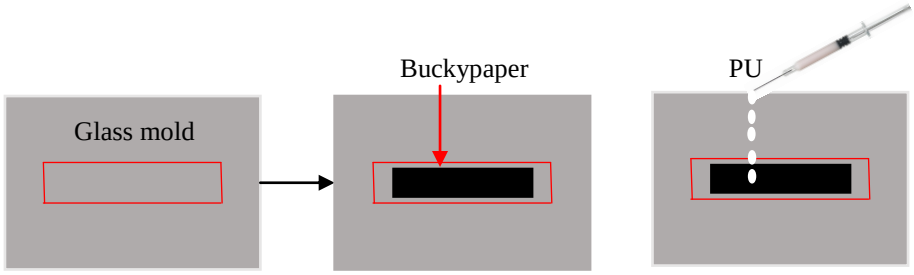

Fig. 1 The Process For Preparation of PU/Buckypaper.

Four grams PU were dissolved into 50 ml Dimethylformamide (DMF). Four ml of PU/DMF were cast in the Buckypaper filled glass mold. Then, the mold was put in 100 °C oven to dry for 5 h. After that, the PU/MWCNT composites were obtained by peeling them off the glass mold. The thickness of the PU is about 80 μm. So, the total thickness of the PU/MWCNTs is around 180 μm. The process is briefly shown in **Figure 1**.

B. Sample Setup For Free Vibration Tests

B.1. Single Side Attachment Mode

The first single side attachment mode was aimed to compare the differences in performance among pure PU, Buckypaper and PU/Buckypaper composites. Firstly, 3.5 cm × 0.9 cm (length × width) of pure PU, Buckypaper and PU/Buckypaper with 80 μm, 100 μm and 180 μm in thickness, respectively, were attached to 9.5 cm × 0.9 cm × 0.048 cm aluminum base beam single side by a thin layer of adhesive(see **Figure 2)**. Three very thin layers of nonconductive 3M CA100 liquid instant adhesive were used to cover these samples to separate the samples from the environment. Each specimen was dried in room temperature for 24 hrs. The base beam material used was 6061-T6 Aluminum. The red dashed lines shown in **Figure 3** defined the two possible locations where the beam was clamped. The side of the

ISSN(Online): 2319-8753
ISSN (Print): 2347-6710

International Journal of Innovative Research in Science, Engineering and Technology

(An ISO 3297: 2007 Certified Organization)

Vol. 4, Issue 12, December 2015

Aluminum base beam without the attachment of samples were tested then cut 1 cm at a time and the results were compared. The unclamped side was then made to vibrate and the damping ratio was determined.

The second single side attachment mode was built to investigate how the damping changed as a function of the coverage of PU/Buckypaper to aluminum base beams. The PU/Buckypaper with dimension of 3.5 cm × 0.9 cm × 0.018 cm was attached upon a 20.5 cm × 0.9 cm × 0.048 cm Aluminum base beam on one side (see **Figure 3**) using a thin layer of glue as discussed in the previous paragraph. The specimen was dried at room temperature for 24 hrs. Free vibration comparisons were made by using either the sample side, #, or the uncovered side, *, alternately, as the fixed support for the cantilever beam. The red dashed lines shown in **Figure 3** defined the locations where the beam was clamped. The side of the Al base beam without the attachment of samples were either cut or clamped 1 cm at a time until the clamp was next to the sample. The unclamped side was then made to vibrate and the damping ratio was determined and the results were compared.

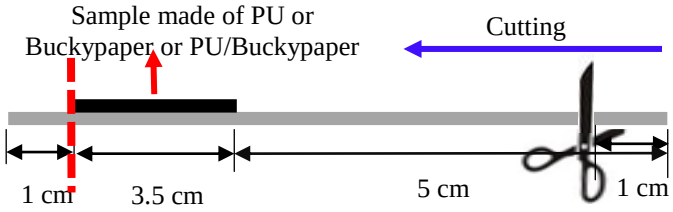

Fig. 2 Schematic Images of Single Side Attachment. The dimension of samples, Al beams and the locations where samples were attached, the locations (red line) where the beam was clamped and also the directions and lengths for beam removal.

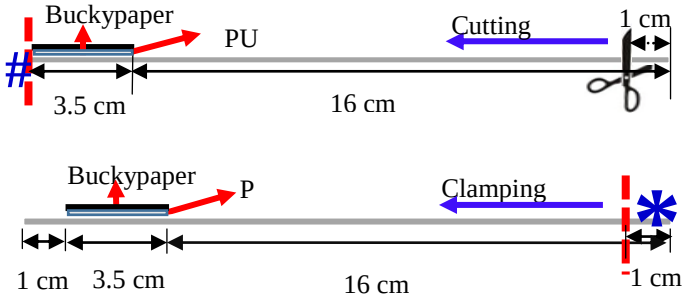

Fig. 3 Schematic Images of Single Side's Attachment. The dimension of samples, Al beams and the locations where samples were attached, the locations of sample side # and free end side * where the beam was clamped and also the directions and lengths for both beam removal and clamping.

B.2. Both Sided Attachment Mode

All the dimensions of sample and aluminum base beams, the clamped locations and the directions and lengths for both cutting and clamping are kept the same as the second single side attachment mode described above. The only change that was made was that the aluminum base was covered on both sides by the sample (See **Figure 4).**

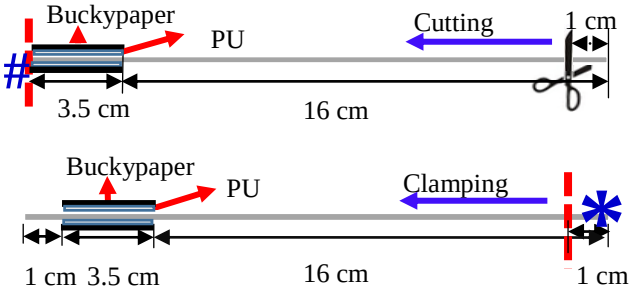

Fig. 4 Schematic Images of Double Sides' Attachment. The dimension of samples, Al beams and the locations where samples were attached, the locations of sample side # and free end side * where the beam was clamped and also the directions and lengths for both beam removal and clamping.

ISSN(Online): 2319-8753
ISSN (Print): 2347-6710

International Journal of Innovative Research in Science, Engineering and Technology

(An ISO 3297: 2007 Certified Organization)

Vol. 4, Issue 12, December 2015

C. Damping Test Methodology

The cantilever beams of **Figs. 2, 3 and 4** were given the same, small initial displacement and then released for free vibration. Unclamped end displacements were measured by a laser vibrometer and a two channels digital oscilloscope was used display and store the signal. Five trials were made for each setup and the mean value of the damping ratio was calculated. This ratio can be related to the logarithmic decrement of consecutive maxima of end displacements and can be correlated to how much vibration energy is removed from the sample. The higher the damping ratio, the better the sample acted as a damper.

D. Sample Setup For Drift, Static Tensile Test, and Dynamic Tests

The sensor was bonded to the center of a 50 mil thick 6061-T6 Aluminum rectangular bar using 3M CA100 liquid instant adhesive. Each specimen was held in place by a weight and dried in room temperature for 24 hrs. The bonding area was prepared to ensure a smooth surface, as is normally defined for a foil strain gage, with no oxide formations on the surface. A foil strain gage, Omega SGD-30/350-LY40, 3 cm long x 0.3 cm wide, was bonded to the opposite side of the substrate. 24 AWG solid wire was used to connect decade resistor boxes manufactured by Eisco Labs in a Wheatstone bridge setup for the sensor or the foil strain gauge. Prior to testing, resistance of the sensor and strain gage was measured and the corresponding decade resistance boxes were set to match. The decade resistor boxes have a resolution of about 1 Ohm. This causes the initial millivolt potential different to rarely start at zero. To compensate for this, where appropriate, data points were shifted to allow for comparison of different sensors. Constant voltage was provided during testing by B&K precision power supply (1745A). The voltage supply was set to 5 volts for measured resistance above 20 Ohms. For resistance below 20 Ohms, the voltage supply was set to 2 volts. Signals from the drift and strain measurement tests were collected using National Instruments NI cDAQ-9172 board and LabView software. Signals from the Dynamic sensing tests were collected using Data Translation DT9837C and SpectraPLUS-DT. Linearity and sensitivity of the sensor were evaluated using quasi-static loadings. These loadings were carried out using a United SSTM-2K model tensile test machine.

E. Drift Test Procedures

The mounted sample was connected to the measurement system and placed in a no load and ambient temperature condition for at least 24 hours prior to testing. The test equipment was then turned on, and at least 30 minutes of data were collected for each sample. The drift test was performed several times for the sake of repeatability.

F. Static Test Procedures

The mounted sample was placed in the tensile testing machine and connected to the measurement system. The system was left idle for at least 1 hour prior to testing in order to remove any accumulated stresses due to mounting. Signal collection was initiated. The tensile test system was set to extend at a rate of 0.001"+/-0.0005" per minute. This way the system was considered to be operating quasistatically. The system was set to increase ramp force at the set extension rate until 400 lbs of force was achieved. The system was then set to instantaneously reduce load to 0 lbs. This procedure was repeated multiple times to determine repeatability of the results and hysteresis in the system.

G. Dynamic Test Procedures

The sample was mounted onto a cantilever beam system. The sensor was located as close as possible to the fixed end. The free end was attached to a vibration drum that vibrates at specified frequencies. An accelerometer was attached to the free end, as close to the center of the vibration drum as possible. The accelerometer linked into a feedback loop that ensured that the acceleration of the free end was correct as per the frequency versus acceleration profile. This profile was set up such that the acceleration started at 10 Hz and 10 g's, ramped up to 20 Hz and 20 g's, then held a constant acceleration of 20 g's from 20 Hz to 6000 Hz. The control system was then set to run a specified frequency or swept across a range of frequencies. The resulting signals were collected and analyzed using the Hanning FFT algorithm. The peak hold data for the signals were collected over the course of 500 signal samples using a sampling rate of 11000 Hz for an input frequency range of 10 to 1000 Hz and 60000 Hz for an input frequency range of 1000 to 5000 Hz. Five sets of peak hold data were taken and analyzed.

ISSN(Online): 2319-8753
ISSN (Print): 2347-6710

International Journal of Innovative Research in Science, Engineering and Technology

(An ISO 3297: 2007 Certified Organization)

Vol. 4, Issue 12, December 2015

III. RESULTS AND DISCUSSION

A. Damping Ratios of PU, Buckypaper and PU/Buckypaper Composites

The free end vibration test has already shown that the Buckypaper has strain sensing properties [11]. Also, PU has excellent damping ability which is broadly studied. Herein, the free end vibration test method was adopted to study the damping behaviors of PU, Buckypaper and their layer by layer PU/Buckypaper composite. For the Al base beam the single side attachment test free vibration trial results are shown in **Figure 5** (see **Figure 2** for the configuration of the tests setup)**.** Many tests were run and no delamination in the PU/Buckypaper composites was observed in any of the specimens used.

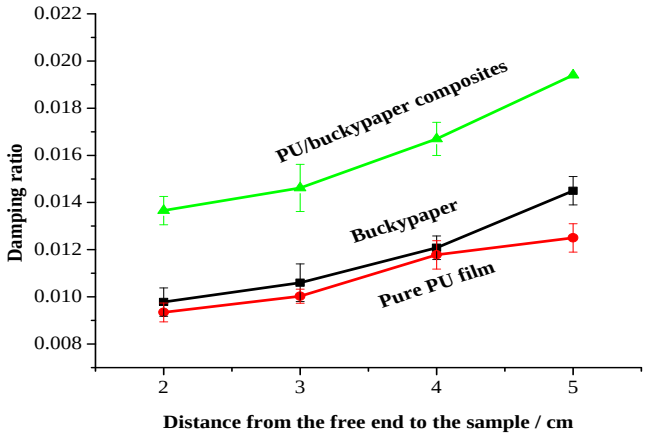

Fig. 5 Damping Ratios Comparison of PU, Buckypaper and PU/Buckypaper Composites.

B. Damping Results For Single Side Attachment

As mentioned previously, the reason for the creation of the composite is for use as a sensor-actuator with damping capabilities. To check on the damping capability aspect, several tests were performed. For the Aluminum base beam single sided attachment test (see **Figure 3** for the configuration of the tests setup), free vibration trial results are shown in **Figure 6.**

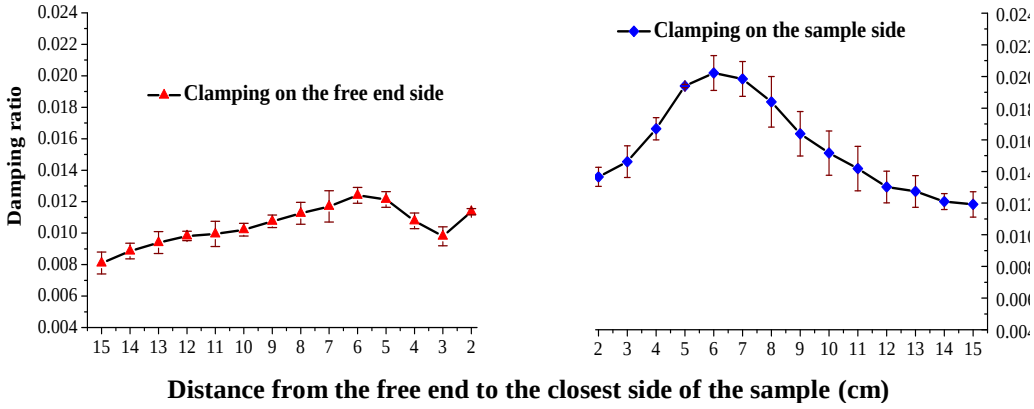

Fig. 6 Damping Ratios of Single Side Attached PU/Buckypaper Clamped On The Free End * Side and The Sample # Side.

Five trials were run for each of clamping listed. The results clearly showed that the damping ratio initially increased as the distance from the free end to the sample decreased for both clamping on the free end side * and clamping on the sample side # (see **Figure 6**). Then, it decreased as the distance from the free end to the sample further decreased for

ISSN(Online): 2319-8753
ISSN (Print): 2347-6710

International Journal of Innovative Research in Science, Engineering and Technology

(An ISO 3297: 2007 Certified Organization)

Vol. 4, Issue 12, December 2015

both clamping on the free end side * and clamping on the sample side #. For both clamping on the free end side * and clamping on the sample side #, the damping ratio reached the highest values 0.0124 and 0.0202, respectively, when the distance from the free end to the sample is 6 cm. Comparing the highest damping ratios, 0.0124 and 0.0202, when the distance from the free end to the sample is the same 6 cm, it is determined that clamping on the sample side # has 162.9% higher damping ratio than when clamping on the free end side *. The trends follow previous published results for constrained layer viscoelastic dampers.

There is a further increase of the damping ratio after it decreases for the case where the clamping is on the free end side *. This is reasonable when compared with the trend of the damping ratio of clamping on the sample side. The damping ratios remain lower for each new beam length trial when clamped on the free end side compared with the value for each beam length trial when clamped on the sample side. However, the damping ratios have to be the same when the beam being tested becomes symmetric with respect to the vertical axis; meaning, it doesn't matter whether you test the clamped side or the free end side, both will be the same configuration leading to the same damping ratio.

C. Damping Results For Single Side Attachment

The double sides' attachment setup which is shown in **Figure 4** displays the same trend of damping ratios as single sided attachment (See **Figure 7)**. However, the double sided attachment has higher damping ratios compared with single side attachment. It reaches the highest damping ratio of 0.033 with double sides' attachment when the sample's right end is 3 cm away from the free end. Also, the damping ratios differences between clamping on the sample side and clamping on the free end with the same distance from the free end to the sample is bigger for double sided attachment than the single sided attachment. An increase in damping ratio when clamped on the free end side is noted, which is just like the single side attachment trend. The Y-coordinate value is very close at the 0 cm value of X-coordinate, which is expected.

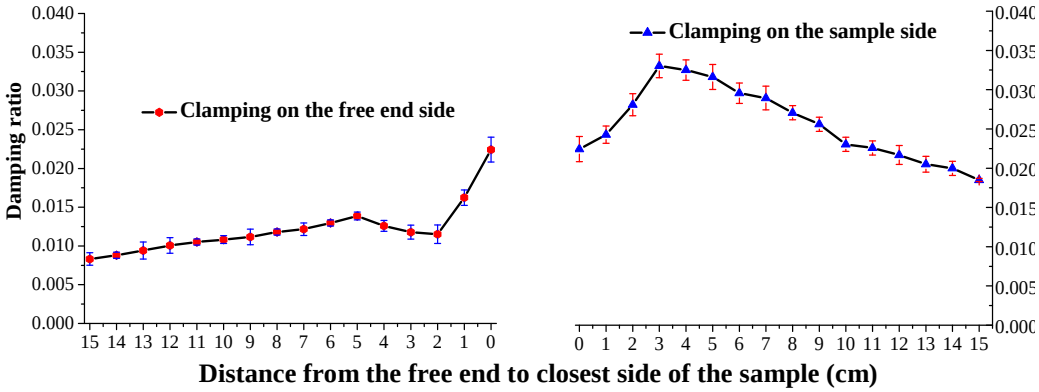

Fig. 7 Damping Ratios of Double Sides Attached PU/Buckypaper Clamped On The Uncovered * Side and Sample # Side.

When one compares the loss factor as a function of the non-dimensional coverage length in both these cases, the graphs of **Figure 8** are obtained. Here, the loss factor, η, is twice the damping ratio for small damping ratios up to 0.3 [7]. We note the similarity in trends of the loss factor for the sample side clamping condition, #, when compared to Chen and Levy [7]. First the double sided coverage produces a higher loss factor which increases as the sample length to the beam length (L1/L) increases and then begins to decrease as L1/L tends to 1.

An analysis of the loss factor versus non-dimensional coverage length when clamping is on the free end side, *, is now undertaken. This analysis applies for the single side and also for the double side coverage, as well. The loss factor for small L1/L can best be described as that for a sample starting to act as a passive layer type damping element and as an end mass. But as the beam material is removed, thereby increasing L1/L, the loss factor of the sample transitions to more of a loss factor for a passive layer type damping element covering more and more of the beam. We note that the loss factor, η, first increases with coverage length, L1/L, though its value is several times smaller than its value when the beam is clamped on the sample side. In this configuration the sample acts as a small mass at the end of the beam

ISSN(Online): 2319-8753
ISSN (Print): 2347-6710

International Journal of Innovative Research in Science, Engineering and Technology

(An ISO 3297: 2007 Certified Organization)

Vol. 4, Issue 12, December 2015

and coverage length effects dominate. Then the loss factor decreases to a minimum value before increasing again as L1/L, the dimensionless coverage length, increases. This decrease may be due to the fact that as more beam is removed, the sample starts to act as a larger end mass compared to the mass of the beam and that becomes the dominating effect. Such a system will tend to execute relatively larger end displacements, and, according to Rao [12], for viscoelastic materials, this implies a lower loss factor (see [12], pg. 686). As more beam material is removed, a second increase occurs in the loss factor due to the sample transitioning from being like an end mass to beginning to cover the majority of the beam. This behavior is similar to that found in Chen and Levy [7] for the vibration of a viscoelastic constrained layer damping of a beam with end mass. However, this increase-decrease-increase phenomenon in the loss factor is noticed for both the single side and double side coverage of the beam. Though [13] [14] investigated the change in L1/L by increasing L1 and keeping L fixed, the behavior seen in this investigation can be deduced from the results found in [13] [14] and follow the trends therein. However, the differences in loss factor between single sided and double sided coverage were much larger in [13] compared to what is noted here because of the materials used. Yet, the trends in [13] and shown in this work are very similar.

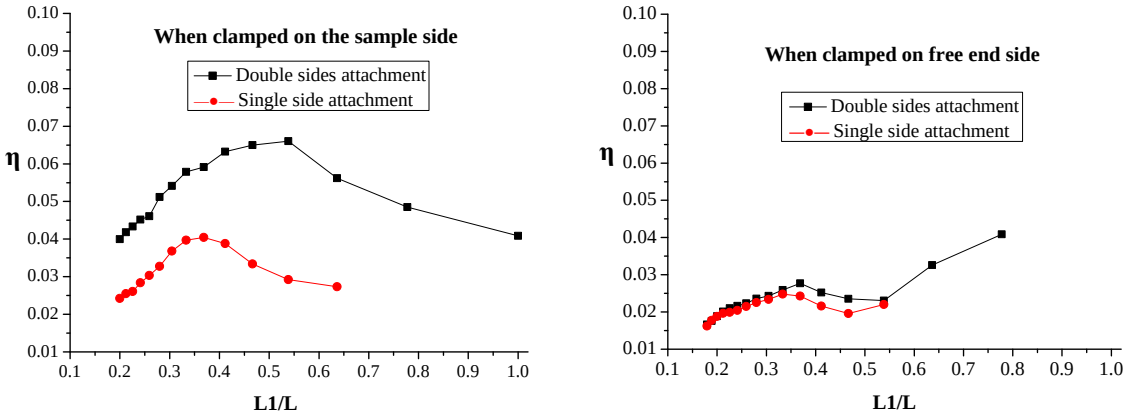

Fig. 8 Comparison Between Single Side and Double Sided Attachment of The PU/Buckypaper Sample For Both Clamping Conditions

IV. STATIC SENSING PROPERTIES

A. The Drift Effect

The stability of each sensor was tested and typical results for some samples and strain gage are shown below. The drift test was executed for the sample and for the strain gage for a period of 30 minutes or more. The voltage data were captured and for the sensors were shifted so that average recorded signal value was zero. This allowed for direct comparison of the sensors on the graph. The change in voltage per hour for typical results are also tabulated below. The correlation of the data are small because significant noise was generated in the results due to the high sampling rate. Therefore, other measurements given in succeeding sections do not include the correlation values.

Table 1 Trend Line Slopes and R-values

Type of Sample	Δ mV/hour	R^2
PU/Buckypaper-blue line	-0.6184 mV/h	0.0353
PU/Buckypaper-black line	-1.7925 mV/h	0.0437
Strain Gauge-green line	0.0866 mV/h	0.0003

Figure 9a shows typical results for one strain gage and two sample sensors. We note that the strain gage showed almost no changes over the test period though there is a slight downward slope to the line. The sample sensors also exhibited

ISSN(Online): 2319-8753
ISSN (Print): 2347-6710

International Journal of Innovative Research in Science, Engineering and Technology

(An ISO 3297: 2007 Certified Organization)

Vol. 4, Issue 12, December 2015

very small slopes as well. Figures 9b and 9c show actual traces for one of the samples and the strain gage where the sensor voltage changes by -0.6184 mV/hr while the foil strain gage changes by -0.0866 mV/hr. The final results of this testing showed that some samples were unstable and had significant drift while others were much more stable but consistently had a drift that was one order of magnitude larger than that of the strain gage. This is reasonable since our testing apparatus could not be moved and had no way of isolating our samples from outside vibrations. Foil strain gages are known to be stable in this type of environment.

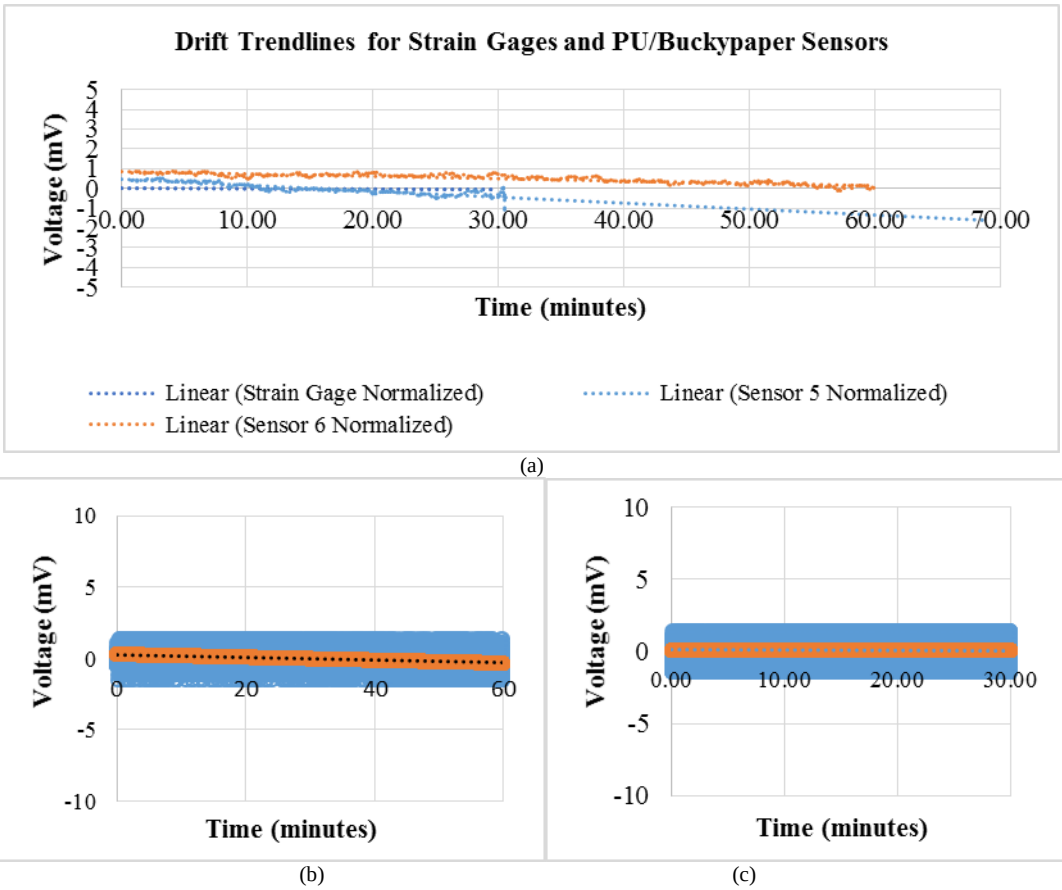

Fig. 9 PU/Buckypaper Sensor and Strain Gage Drift Test (a) Drift trendlines for typical PU/Buckypaper sensor and strain gage; (b) Drift test for PU/Buckypaper sample (sensor 5) and (c) Drift test for strain gage.

B. Linearity and Repeatability - Static Tensile Test

Linearity and repeatability are two very important characteristics for strain sensors. It is desirable that the relationship between the applied strain and the output voltage be linear. The source voltage for the sensor and strain gage in **Figure 10** are equivalent.

Figure 10 shows typical data for a specific sample that responded as desired. This specific dataset shows two quasi-static loadings and instantaneous unload cycles. **Figure 10** provides typical data obtained from testing both the sample sensor and the strain gauge. Provided are the first loading tensile test in which the strain sensing behavior of PU/Buckypaper composites sensor is similar to the behavior of the conventional foil strain gage. Generally, both the sensor's and the strain gage's electric resistance change is essentially linear to the applied strain and is related to the gage factor. The first 4 minutes of the test indicate that the system had a residual strain that required both the sensor and strain gage to adapt to before the test was begun. The second loading occurred about 30 seconds after releasing the previous load. Again, a "no load" time period between the 10th and the 13th minute was introduced before the loading

ISSN(Online): 2319-8753
ISSN (Print): 2347-6710

International Journal of Innovative Research in Science, Engineering and Technology

(An ISO 3297: 2007 Certified Organization)

Vol. 4, Issue 12, December 2015

was begun again. The strain gage appears to have returned to "zero" but the PU/Buckypaper sensor appears to lag behind and shows some hysteresis. The conventional foil strain sensor responded quickly according to the load applied to the beam. However, PU/Buckypaper composites sensor did not completely return to "zero".

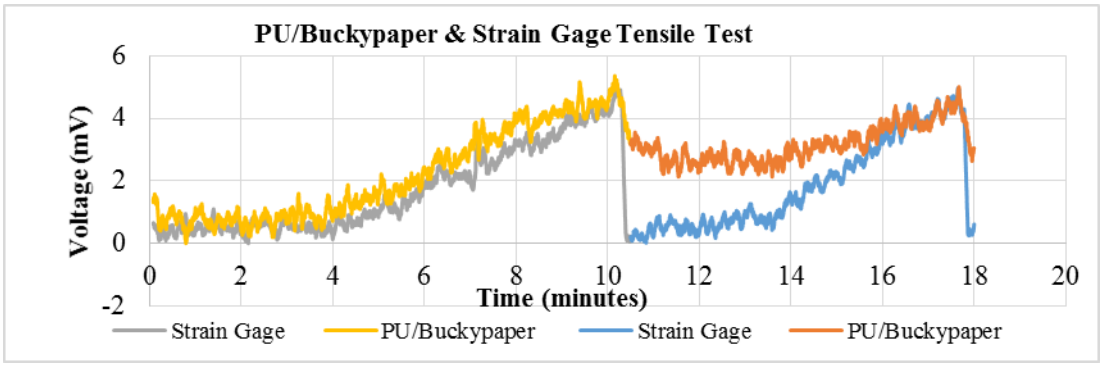

(a)

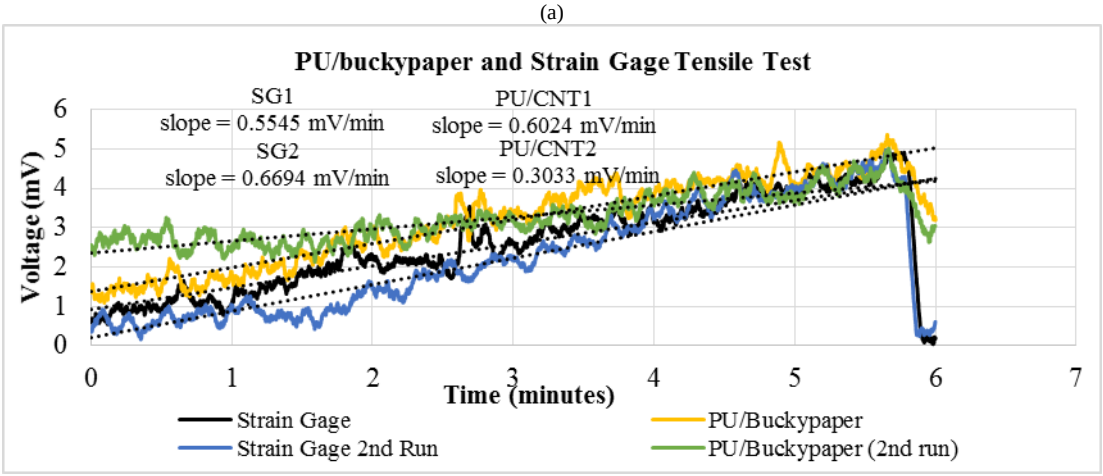

(b)

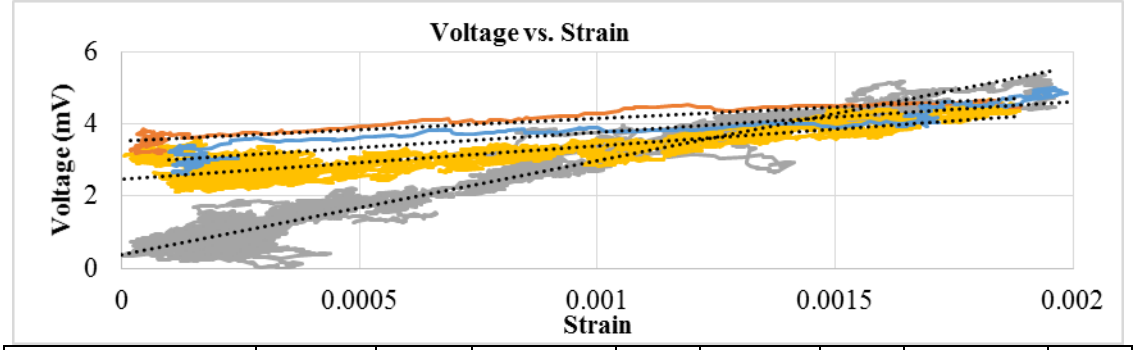

Slope mV/ (m/m)	Load1	2600	Unload1	640	Load2	932	Unload2	857

(c)

Fig. 10 Tensile Test Data and Analysis (a) The repeat loading comparison of PU/Buckypaper and standard foil strain gage-the raw data (b). The repeat loading comparison of PU/Buckypaper and standard foil strain gage-data linearity (c). The loading/unloading comparison of PU/Buckypaper versus strain--first load (gray)/unload (red) and second load (yellow)/unload (blue) of the sensor.

As a new load was applied increasing the strain, the PU/Buckypaper composite sensor responded and sensed the strain linear with the input. Yet, the slope for the sensor appears to be different than during the first load cycle. Hence, both

ISSN(Online): 2319-8753
ISSN (Print): 2347-6710

International Journal of Innovative Research in Science, Engineering and Technology

(An ISO 3297: 2007 Certified Organization)

Vol. 4, Issue 12, December 2015

sensors have a linear voltage output. By factoring out the lag in response of the second loading, all four output trend lines are deemed relatively parallel (**Figure 10(b)**). Additionally, **Figure 10(c)** gives the voltage response relative to strain as well and the slopes of those lines for both types of sensors. Since the input voltage and output voltage are equivalent or relatively similar, so are the gage factors. Therefore, the PU/Buckypaper composite sensor senses similarly to the conventional foil strain gauge in terms of repeatability and linearity.

V. DYNAMIC SENSING CHARACTERISTIC

Dynamic response performance is the importance criterion for sensors. Standard foil strain gages are used for comparison. Herein, the frequency sweep method was used to study the sensitivity of the PU/Buckypaper and the foil strain gages to input frequencies. Frequency domain from 10 Hz to 1000 Hz was investigated and the results are presented in **Fig. 11**. The FFT graphs consistently showed a response at 60 Hz of 0.418 mV for the PU/Buckypaper composite sensor and 1.47 mV for the foil strain gage. This response is due to background source that is always present and can be disregarded. The results displayed in **Figs. 11(a)-(n)** are typical results for the sensor and strain gage.

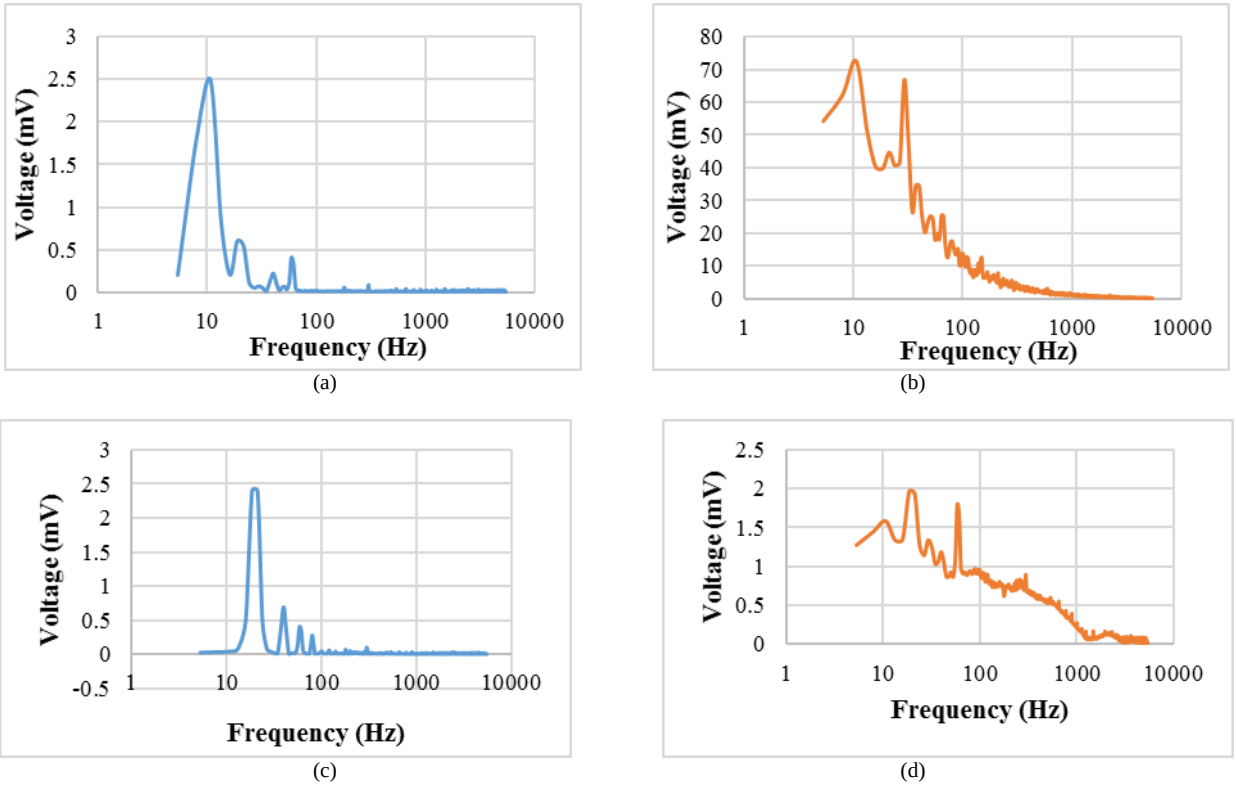

Fig. 11 Comparison of Frequency Response of the Standard Foil Strain Gages and of the PU/Buckypaper. (a) 10 Hz – PU/Buckypaper – Magnitude: 2.4727 mV; (b) 10 Hz – Foil Strain Gage – Magnitude: 70 mV; (c) 20 Hz – PU/Buckypaper – Magnitude: 2.4082 mV; (d) 20 Hz – Foil Strain Gage – Magnitude: 1.9579 mV

ISSN(Online): 2319-8753
ISSN (Print): 2347-6710

International Journal of Innovative Research in Science, Engineering and Technology

(An ISO 3297: 2007 Certified Organization)

Vol. 4, Issue 12, December 2015

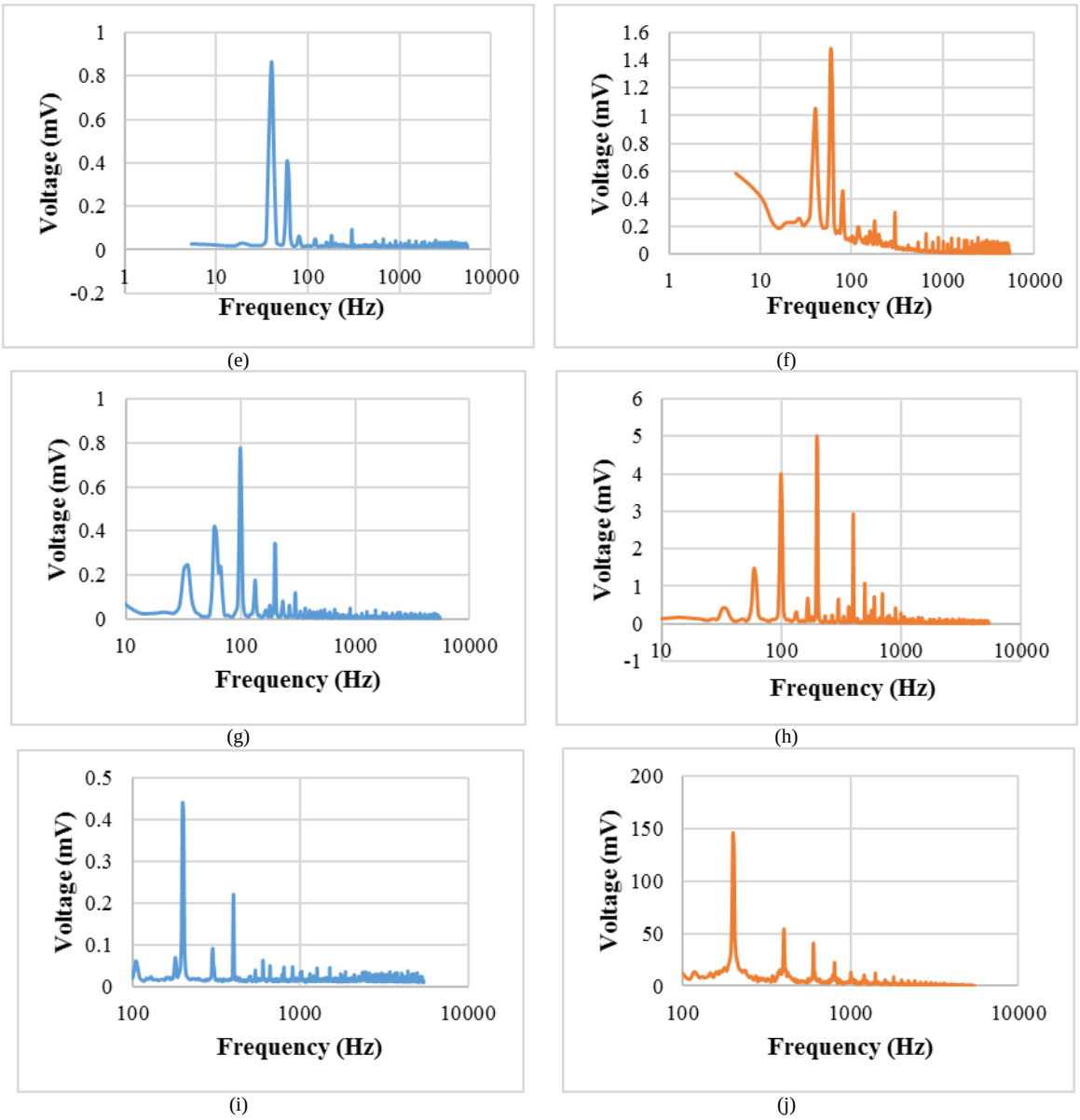

Fig. 11 Comparison of Frequency Response of the Standard Foil Strain Gages and of the PU/Buckypaper. (e) 40 Hz – PU/Buckypaper – Magnitude: 0.8601 mV; (f) 40 Hz – Foil Strain Gage – Magnitude: 1.0515 mV; (g) 100 Hz – PU/Buckypaper – Magnitude: 0.7716 mV; (h) 100 Hz – Foil Strain Gage – Magnitude: 3.9748 mV; (i) 200 Hz – PU/Buckypaper – Magnitude: 0.4374 mV; (j) 200 Hz – Foil Strain Gage – Magnitude: 145.43 mV

Shown in **Figs. 11(a)-11(j)**, over the range of 10 Hz to 200 Hz, the PU/Buckypaper composite sensor is either the same or is superior to the normal foil strain gage for sensing purposes since the highest peak consistently corresponds to the input frequency. The foil strain gage is superior at 10 Hz and 200 Hz in the sense that it gives a significantly larger voltage response when compared to the composite sensor. In higher frequencies, the composite sensor either performed better or both signals were not detectable to any accuracy for sensing.

ISSN(Online): 2319-8753
ISSN (Print): 2347-6710

International Journal of Innovative Research in Science, Engineering and Technology

(An ISO 3297: 2007 Certified Organization)

Vol. 4, Issue 12, December 2015

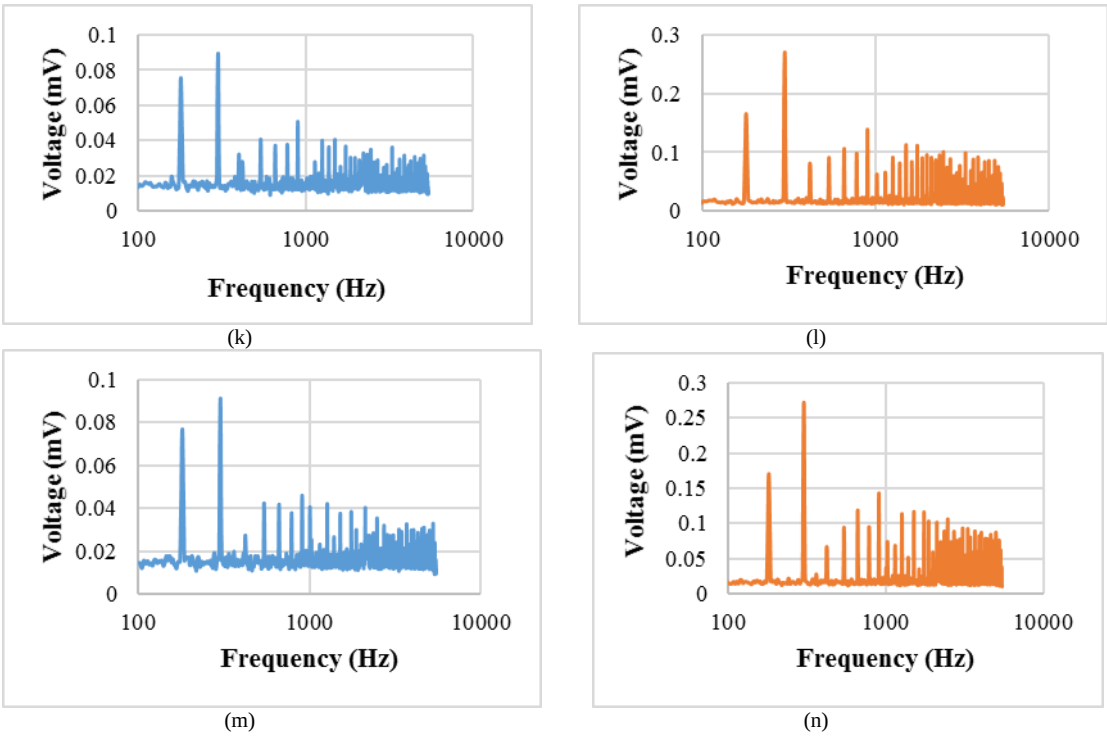

Fig. 11 Comparison Frequency Response of the Standard Foil Strain Gages and of the PU/Buckypaper. (k) 400 Hz – PU/Buckypaper – Magnitude: 0.0325 mV; (l) 400 Hz – Foil Strain Gage – Magnitude: 0.0229 mV; (m) 1000 Hz – PU/Buckypaper – Magnitude: 0.0403 mV; (n) 1000 Hz – Foil Strain Gage – Magnitude: 0.0365 mV

When the frequency is increased, the voltage output for both strain gage and PU/Buckypaper composites decreases greatly. The voltage output of PU/Buckypaper composites dropped to 0.77 mV with frequency of 100 Hz and the strain gage drops to about 3.98 mV. When the frequency is further increased to 1000 Hz, the voltage output of both sensors remain of the same order, 0.0403 vs. 0.0365 mV. It means that the PU/Buckypaper composites strain sensors may be better for structural health monitoring, which frequently uses the change of the natural frequency as an index for detecting small cracks (e.g., [15-17]).

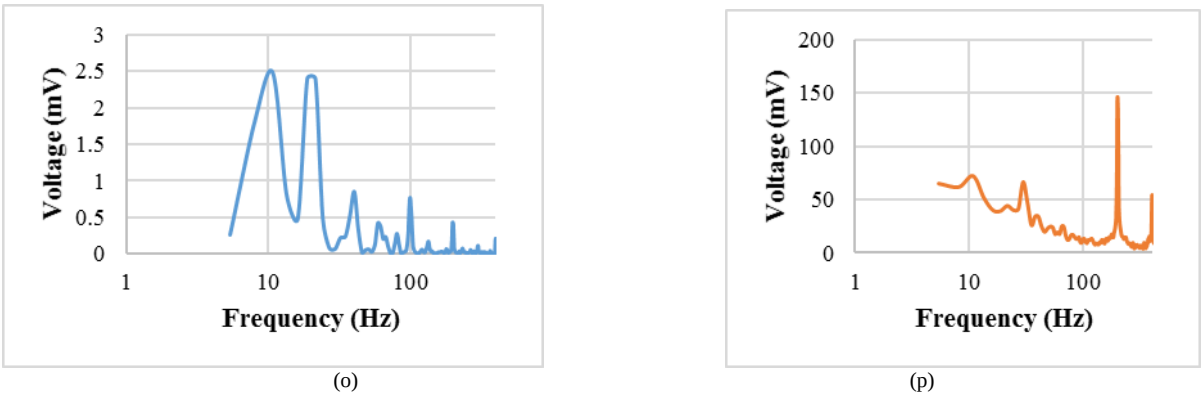

Fig. 11 Comparison of Frequency Response of the Standard Foil Strain Gages and of the PU/Buckypaper. (o) FRF superposition-PU/Buckypaper sensor (10-400 Hz); (p) FRF superposition – Foil strain gage (10-400 Hz)

Figures 11(o) and (11p) are the superposition of the FRFs shown in **Figs. 11 (a)-(n)** and represent the response of

ISSN(Online): 2319-8753
ISSN (Print): 2347-6710

International Journal of Innovative Research in Science, Engineering and Technology

(An ISO 3297: 2007 Certified Organization)

Vol. 4, Issue 12, December 2015

PU/Buckypaper or of the strain gage, respectively, to the different input frequencies. This is not a true FRF because the frequency sweep method must be used to generate these graphs. The graphs show a fuller picture of the dynamic sensing capabilities of each sensor. This is advantageous for the comparison of the sensor and strain gage because it shows how the signal could be used for frequency sensing. The graph for the PU/Buckypaper composite sensor shows a sensor that responds to frequencies in the range of 10 to 200 Hz while at the same time having each frequency signal distinguishable from each other. The foil strain gage does not have this capability. The 10 Hz foil strain gage response eclipses all the frequency responses up to 200 Hz and appears to show a peak at 30 Hz, a frequency for which no sampling was made. For the reasons stated, the PU/Buckypaper composite sensor responds in a superior manner when compared to a foil strain gage.

VI. CONCLUSION

A PU/Buckypaper sensor was created to evaluate its sensing and damping capabilities versus a standard foil strain gage and constrained layer damping system. The free end vibration test results showed that for the single side attachment, the damping ratios for both PU film and Buckypaper are close, while PU/Buckypaper composites have higher damping ratios than their individual components. For both single side attachment and double sided attachment, the damping ratios when clamping on the sample side are much higher than when clamping on the free end side.

The relationship of loss factor, η, and beam coverage L1/L was discussed for single sided and double sided attachment. Briefly, the loss factor, η, increases with coverage length L1/L increases. The loss factor, η, then decreases before increasing again as the coverage length L1/L continues to increase. The trend for double sided attachment is found to follow the trends discussed by Rao [12] and Levy and Chen [14].

The possibility of PU/Buckypaper to be used as a strain sensor was also investigated. Though, there is a drift for the PU/Buckypaper sensor during the one hour long drift test, the slope is relatively small.

Two loading cycle tests showed that though there are residual strain for both PU/Buckypaper sensor and standard foil strain sensor for both loading cycles, the PU/Buckypaper sensor appears to lag behind and shows some hysteresis in the second loading cycle. However, both sensors had a linear voltage output and all four output trend lines are deemed relatively linear and in the first cycle also parallel. Therefore, the PU/Buckypaper composite sensor senses similarly to the standard foil strain gauge in terms of repeatability and linearity.

The dynamic sensing test results showed that over the range of 10 Hz to 200 Hz, the PU/Buckypaper composite sensor was comparable to or superior for sensing purposes since the highest peak consistently corresponded to the input frequency. In higher frequencies, the composite sensor either performed better or both signals were not detectable to any accuracy for sensing. It means that the PU/Buckypaper sensor has the potential to be strain sensor.

Lastly, not all samples created were capable sensors. However, the ones that worked produced repeatable results. In comparison to viscoelastic (VEM) constrained layer dampers discussed in [13] [14], the same size PU/Buckypaper sensor would have a density that is 40% of the VEM and 6.4% of the density of the constraining layer, would have similar damping behavior, but would have more useful attributes for a sensor.

CONFLICT of INTEREST

The authors declare that they have no conflict of interest related to this work.

ACKNOWLEDGEMENT

The authors are grateful to the US Army Research Laboratory and US Army Research office for the following Grant No. 58940-RT-REP that enabled this work to be possible. One author (HF) thanks Florida International University for the Dissertation Year Fellowship which allowed for his participation in this work.

ISSN(Online): 2319-8753
ISSN (Print): 2347-6710

International Journal of Innovative Research in Science, Engineering and Technology

(An ISO 3297: 2007 Certified Organization)

Vol. 4, Issue 12, December 2015

REFERENCES

[1] Magalhães, F., Cunha, A., and Caetano, E., "Vibration based structural health monitoring of an arch bridge: From automated OMA to damage detection", Interdiscip Integr Asp Struct Health Monit, Vol. 28, pp. 212–28, 2012.
[2] Wahalathantri, B. L., Thambiratnam, D. P., Chan, T. H. T., Fawzia, S., "Vibration based baseline updating method to localize crack formation and propagation in reinforced concrete members", J Sound Vib, Vol. 344, pp. 258–76, 2015.
[3] Lu, Z. R., and Liu, J. K., "Identification of both structural damages in bridge deck and vehicular parameters using measured dynamic responses", Comput Struct, Vol. 89:, pp. 1397–405, 2011.
[4] Koratkar, N., Wei, B. Q., and Ajayan, P. M., "Carbon Nanotube Films for Damping Applications", Adv Mater, Vol. 14, pp. 997–1000, 2002.
[5] Zhou, X., Shin, E., Wang, K. W., and Bakis, C. E., "Interfacial damping characteristics of carbon nanotube-based composites", Dev Carbon Nanotube Nanofibre Reinf Polym, Vol. 64, pp. 2425–37, 2004.
[6] Xiong, J., Zheng, Z., Qin, X., Li, M., Li, H., and Wang, X., "The thermal and mechanical properties of a polyurethane/multi-walled carbon nanotube composite", Carbon, Vol. 44, pp. 2701–7, 2006.
[7] Buffa, F., Abraham, G. A., Grady, B. P., and Resasco, D., "Effect of nanotube functionalization on the properties of single-walled carbon nanotube/polyurethane composites", J Polym Sci Part B Polym Phys, Vol. 45, pp. 490–501, 2007.
[8] Li, X., Levy, C., and Elaadil, L., "Multiwalled carbon nanotube film for strain sensing", Nanotechnology, Vol. 19, pp. 045501, 2008.
[9] Sasikumar, K., Manoj, N. R., Ramesh, R., and Mukundan, T., "Carbon nanotube-polyurethane nanocomposites for structural vibration damping", Int J Nanotechnol , Vol. 9, pp. 1061–1071, 2012.
[10] Li, L., Tian, B., Zheng, Y., Wang, Y., Chen, F., Tong, Y., and Liu, E. B., "Method for preparing NiTi spring-carbon nanotube-polyurethane composite damping materials", 2014.
[11] Li, X., and Levy, C., "A Novel Strain Gauge with Damping Capability", Sensors and Transducers Journal, Special Issue-MEMS: from Micro Devices to Wireless Systems, Vol. 7 (10), pp. 5-14, 2009.
[12] Rao, S. S., "Mechanical Vibrations", 4th Edition, Pearson-Prentice Hall, pp. 150 and pp. 686, 2004.
[13] Chen, Q., and Levy, C., "Vibration Characteristics of a Partially Covered Double Sandwich Cantilever Beam", AIAA Journal, Vol. 34, pp. 2622-2626, 1996.
[14] Chen, Q., and Levy, C., "Vibration Analysis of a Partially Covered, Double Sandwich Cantilever Beam with Concentrated Mass at the Free End", International Journal of Solids and Structures, Vol. 31, pp. 2377-2391, 1994.
[15] Li, X., Levy, C., Agarwal, A., Datye, A., Elaadil, L., Keshri, A. K., and Li, M., "Multifunctional carbon nanotube film composite for structure health monitoring and damping", The Open Construction and Building Technology Journal, Vol. 3, pp.146-152, 2009.
[16] Soyoz, S., and Feng, M. Q., "Instantaneous damage detection of bridge structures and experimental verification", Structural Control and Health Monitoring, Vol.15(7), pp.958-973, 2008.
[17] Kai, H. H., Marvin, W.H., and Paul, J.B., "Overview of vibrational structural health monitoring with representative case studies", Journal of Bridge Engineering, Vol.11(6), pp.707-715, 2006.